Coulomb correlations in quantum wires in strong magnetic fields and their contribution to the Fermi-edge group velocity

2001 J. Phys.: Condens. Matter 13 1539

(http://iopscience.iop.org/0953-8984/13/7/315)

INSTITUTE OF PHYSICS PUBLISHING JOURNAL OF PHYSICS: CONDENSED MATTER

J. Phys.: Condens. Matter **13** (2001) 1539–1550 www.iop.org/Journals/cm PII: S0953-8984(01)16260-0

Coulomb correlations in quantum wires in strong magnetic fields and their contribution to the Fermi-edge group velocity

Zhongxi Zhang and P Vasilopoulos

Department of Physics, Concordia University, 1455 de Maisonneuve Ouest, Montréal, Québec, Canada, H3G 1M8

E-mail: zxzhang@boltzmann.concordia.ca (Zhongxi Zhang) and takis@boltzmann.concordia.ca (P Vasilopoulos)

Received 10 August 2000, in final form 6 December 2000

Abstract

The screening of the Coulomb interaction in quantum wires, subject to strong perpendicular magnetic fields, is assessed by means of an approximate analytic solution of the integral equation for the screened potential as well as by the numerical solution of this equation. The exchange–correlation contribution to the Fermi-edge group velocity, $v_g^{ec}(k_F)$, is proved to be nonsingular. For sufficiently strong magnetic fields, $v_g^{ec}(k_F)$ is approximately the same as the Hartree velocity $v_g^H(k_F)$. The energy dispersion curves, obtained in the screened Hartree–Fock approximation, agree well with experimental observations.

1. Introduction

In recent years considerable efforts have been devoted to the electron–electron effects on the subband structure of quantum wires (QWs) in the presence of high magnetic fields [1–5]. In submicron-width channels, many-body electron–electron interactions play a very important role. However, to date, we are aware only of Hartree [2, 4] and Hartree–Fock [3] treatments of Landau levels (LLs). In reference [6], correlation effects and their influence on the spin splitting have been studied within the screened Hartree–Fock approximation (SHFA). One important conclusion of this work is that corrections caused by screening strongly suppress the exchange splitting and smooth the energy dispersion near the Fermi edge, where the derivative of the exchange contribution diverges logarithmically. This is similar to the case of a three-dimensional (3D) free-electron gas. As is well known, the unphysical singularity of the Hartree–Fock energy can be traced back to the divergence of the Fourier transform of the bare Coulomb potential $4\pi e^2/q^2$ at $\vec{q} = 0$, and it can be removed by taking into account the screening effects of other electrons in the system. However, in a quantum wire subject to a strong perpendicular magnetic field, it is not clear how the singularity at the Fermi level caused by exchange is cancelled by the screening and what the properties of the screening field are.

0953-8984/01/071539+12$30.00

The derivative, with respect to the wave vector, of the single-particle energy near the Fermi level, i.e. the group velocity, is also worth considering because it is not only closely related to the energy dispersion curves but also connected to experimental results [5].

In reference [6] the correlations were treated by an incomplete iteration procedure and the strong suppression of exchange splitting obtained relied on nonstandard approximations for the energy and group velocity. As discussed in reference [6] the validity of some of these approximations is not obvious for $r_0 \sim 1$. Though the results of reference [6] are reasonable and in agreement with some experimental results [5], it is desirable to have self-consistent results obtained, e.g., by a complete iteration procedure, and obtain as explicit an expression for the group velocity as possible. This is the purpose of the present work and the results are obtained by both a numerical and an approximate analytical solution of the pertinent integral equation for the screened potential. Importantly, our results are obtained without the assumption $r_0 \ll 1$ common to standard perturbative calculations.

In sections 2 and 3 we present the formalism and obtain an approximate analytical solution of the integral equation for the screened potential. This solution agrees well with that obtained by solving the integral equation numerically. In section 4 we use the analytical solution to calculate the correlation energies on the basis of the SHFA. As expected, at the Fermi edge the divergence of the exchange is cancelled exactly by that of the correlations. In addition, we obtain new expressions for the contributions of exchange and correlations to the group velocity at the Fermi edge. Concluding remarks follow in section 5.

2. Basic relations

2.1. Free-particle energies

We consider an electron gas confined in a submicron-width channel, of width W, by a potential V_y and subjected to a strong magnetic field $\vec{B}$ applied along the z-direction. If exchange and correlation effects are neglected, the confining potential V_y can be taken as parabolic [6] for $W < 0.3$ μm, i.e., $V_y = m^*\Omega^2 y^2/2$, where m^* is the effective mass. Then the one-electron Hamiltonian h^0 is given, in the Landau gauge $\vec{A} = (-By, 0, 0)$, by

$$h^0 = [(p_x + eBy)^2 + p_y^2]/2m^* + V_y + g_0\mu_B S_z B/2$$
$$= \frac{p_y^2}{2m^*} + \frac{1}{2}m^*\tilde{\omega}^2[y - y_0(p_x)]^2 + \frac{p_x^2}{2\tilde{m}} + \frac{1}{2}g_0\mu_B S_z B \tag{1}$$

where

$$\omega_c = |e|B/m^* \qquad \tilde{\omega} = (\omega_c^2 + \Omega^2)^{1/2}$$
$$\tilde{m} = m^*\tilde{\omega}^2/\Omega^2 \qquad y_0(p_x) = p_x\omega_c/m^*\tilde{\omega}^2.$$

The corresponding eigenvalues ε_α and eigenfunctions $\Psi_{n,k_x}\Psi_\sigma$ are given by

$$\varepsilon_\alpha \equiv \varepsilon_{n,k_x,\sigma} = \hbar\tilde{\omega}(n + 1/2) + \hbar^2 k_x^2/2\tilde{m} + g_0\mu_B\sigma B/2 \tag{2}$$
$$\Psi_{n,k_x} = \mathrm{e}^{\mathrm{i}k_x x}\Phi_n(y - y_0(k_x))/\sqrt{L}. \tag{3}$$

Ψ_σ is the spin wave function with eigenvalue $\sigma = \pm 1$. For the calculations that follow we need the matrix elements [6] for $L \to \infty$:

$$\langle n'k_x'|\mathrm{e}^{\mathrm{i}\vec{q}\cdot\vec{r}}|nk_x\rangle = \delta_{q_x+k_-,0}(n'k_x'|\mathrm{e}^{\mathrm{i}q_y y}|nk_x)$$
$$= \delta_{q_x+k_-,0}\left(\frac{n'!}{n!}\right)^{1/2}\left(\frac{a(k_x' - k_x) + \mathrm{i}q_y}{\sqrt{2}/l}\right)^{n-n'}\mathrm{e}^{-u/2}L_{n'}^{n-n'}(u)\mathrm{e}^{\mathrm{i}aq_y k_+ l^2/2}. \tag{4}$$

Here $k_\pm = k_x \pm k'_x$, $a = \omega_c/\tilde{\omega}$, $u = [a^2 q_x^2 + q_y^2]\tilde{l}^2/2$, $l = (\hbar/m^*\tilde{\omega})^{1/2}$ is the renormalized magnetic length, and $L_{n'}^{n-n'}(u)$ the Laguerre polynomial. In agreement with experiments [5] we assume that V_y is sufficiently smooth that $\Omega \ll \omega_c$. This means that V_y affects the eigenfunctions very little but it changes the eigenvalues considerably. This condition is usually fulfilled for strong fields B.

2.2. Exchange and correlation corrections

The correction to the single-particle energy due to exchange and correlations, $\varepsilon^{ec}_{n,k_x,\sigma}$, can be obtained by using, e.g., the screened Hartree–Fock approximation (SHFA) [9]. When the upper, spin-split Landau level (LL) ($n = 0, \sigma = -1$) is empty, i.e. for $\nu = 1$, $\varepsilon^{ec}_{0,k_x,1}$ is given by [6]

$$\varepsilon^{ec}_{0,k_x,1} \approx -\frac{1}{8\pi^3}\int_{-k_F}^{k_F} \mathrm{d}k'_x \int_{-\infty}^{\infty} \mathrm{d}q_y \int_{-\infty}^{\infty} \mathrm{d}q'_y \; V^s(k_x - k'_x, q_y, q'_y) \times (0k_x|\mathrm{e}^{\mathrm{i}q_y y}|0k'_x)(0k'_x|\mathrm{e}^{\mathrm{i}q'_y y}|0k_x) \tag{5}$$

where $V^s(q_x, q_y, q'_y)$ is the Fourier transform of the screened Coulomb interaction. As is usual in the SHFA [9], we treat the screened potential ϕ in the static limit. Then V^s in equation (5) obeys the integral equation [6]

$$V^s(q_x, q_y, q'_y) = \frac{v_0\delta(q_y + q'_y)}{q} + \frac{v_0}{8\pi^3 q}\int_{-\infty}^{\infty} \mathrm{d}q_{y1} \; V^s(q_x, q_{y1}, q'_y) \times \sum_{n_\alpha, n_\beta}\int_{-\infty}^{\infty} \mathrm{d}k_{x\alpha} \; F_{\alpha,\beta}(n_\alpha, k_{x\alpha}|\mathrm{e}^{\mathrm{i}q_{y1}y}|n_\beta, k_{x\alpha} - q_x) \times (n_\beta, k_{x\alpha} - q_x|\mathrm{e}^{-\mathrm{i}q_y y}|n_\alpha, k_{x\alpha}). \tag{6}$$

Here $v_0 = 4\pi^2 e^2/\epsilon$ and $k_F = (\tilde{\omega}/\hbar\Omega)[2m^* \Delta E_{F\uparrow}]^{1/2}$ is the characteristic wave vector such that this level is filled only for $|k_x| \leqslant k_F$ ($\Delta E_{F\uparrow} = E_F - \hbar\tilde{\omega}/2 - g_0\mu_B B/2$). Within the random-phase approximation (RPA), the tensor $F_{\alpha,\beta}$ connects the screened field V^s with the induced charge density, or the 'induced' density matrix $\rho^s = \rho - \rho^0$, in the following manner:

$$\langle n_\beta, k_{x_\beta}|\rho^s|n_\alpha, k_{x_\alpha}\rangle = \frac{f_{n_\beta,k_{x_\beta}} - f_{n_\alpha,k_{x_\alpha}}}{\varepsilon_{n_\beta,k_{x_\beta},1} - \varepsilon_{n_\alpha,k_{x_\alpha},1} + \mathrm{i}\hbar/\tau}\langle n_\beta, k_{x_\beta}|V^s|n_\alpha, k_{x_\alpha}\rangle \equiv F_{\alpha,\beta}\langle n_\beta, k_{x_\beta}|V^s|n_\alpha, k_{x_\alpha}\rangle. \tag{7}$$

Here $\tau \to \infty$ is the adiabaticity parameter and ρ^0 satisfies

$$\rho^0|\alpha\rangle = f_\alpha|\alpha\rangle$$

where

$$f_\alpha = 1/[1 + \exp((\varepsilon_\alpha - E_F)/k_B T)]$$

is the Fermi–Dirac function. For a system having spatial homogeneity in the x–y plane, the left-hand side of equation (7) is determined only by the difference between the wave vectors of the two states, and equation (6) can be reduced to the standard Lindhard equation [8].

3. Integral equation

3.1. Approximate analytical solution

The first term on the right-hand side of equation (6) is the bare Coulomb potential; the other terms are caused by screening in the QW. The $F_{0,0}$-term involves transitions and screening

within the lowest occupied LL, whereas the terms $F_{0,n}$ and $F_{n,0}$ ($n = 1, 2, 3, \ldots$) involve interlevel transitions and screening. In strong magnetic fields the total screening contribution is determined mainly by the $F_{0,0}$-term and it is sufficient to replace the sum $\sum_{n_\alpha,n_\beta}^{\infty}$ in equation (6) by just three terms [6, 9]: $F_{0,0}$, $F_{0,1}$, and $F_{1,0}$. This means that we take into account only the intralevel and adjacent-level screening. Further, we split V^s as

$$V^s(q_x, q_y, q_y') = v_0\delta(q_y + q_y')/q + V_c^s(q_x, q_y, q_y') \qquad (q^2 = q_x^2 + q_y^2)$$

and use equation (4) and

$$\varepsilon_{n_\alpha} - \varepsilon_{n_\beta}|_{n_\alpha \neq n_\beta} \approx (n_\alpha - n_\beta)\hbar\tilde{\omega}. \tag{8}$$

Denoting by $\mathrm{sinc}(x)$ the function

$$\mathrm{sinc}(x) = \sin(\tilde{k}_F x)/x$$

we can approximate equation (6), for $T \to 0$ K, by

$$\begin{aligned} V_c^s(q_x, q_y, q_y') = {} & \frac{2v_0^2 v_1 l^2}{8\pi^3}\frac{1}{\tilde{q}\tilde{q}'}\mathrm{e}^{-(2a^2\tilde{q}_x^2+\tilde{q}_y^2+\tilde{q}_y'^2)/4} \\ & \times \left[\cos\tilde{k}_F a(\tilde{q}_y + \tilde{q}_y') - \frac{1}{\tilde{\omega}\hbar l a v_1}(a^2\tilde{q}_x^2 - \tilde{q}_y\tilde{q}_y')\,\mathrm{sinc}(\tilde{q}_y + \tilde{q}_y')\right] \\ & + \frac{2v_0 v_1}{8\pi^3}\frac{1}{\tilde{q}}\int \mathrm{d}\tilde{q}_{y1}\; V_c^s(q_x, q_{y1}, q_y')\mathrm{e}^{-(a^2\tilde{q}_x^2+\tilde{q}_y^2+a^2\tilde{q}_1^2)/4} \\ & \times \left[\cos\tilde{k}_F a(\tilde{q}_y - \tilde{q}_{y1}) - \frac{1}{\tilde{\omega}\hbar l a v_1}(a^2\tilde{q}_x^2 + \tilde{q}_y\tilde{q}_{y1})\,\mathrm{sinc}(\tilde{q}_y - \tilde{q}_{y1})\right]. \end{aligned} \tag{9}$$

Here,

$$\begin{aligned} & \tilde{q}_i = q_i l \qquad i\colon x, y, \ldots \\ & q' = (q_x^2 + q_y'^2)^{1/2} \\ & q_1 = (q_x^2 + q_{y1}'^2)^{1/2}. \end{aligned}$$

The solution of equation (9) for the screened potential $V^s(q_x, q_y, q_y')$ can be sought in the form

$$\begin{aligned} V_c^s(q_x, q_y, q_y') = {} & v_0\Phi(\tilde{q}_x, \tilde{q}_y)\Phi(\tilde{q}_x, \tilde{q}_y')\big[\tilde{k}_1\cos\tilde{k}_F\tilde{q}_y\cos\tilde{k}_F\tilde{q}_y' \\ & + \tilde{k}_2\sin\tilde{k}_F\tilde{q}_y\sin\tilde{k}_F\tilde{q}_y' + \tilde{k}_3(\tilde{q}_x^2 - \tilde{q}_y\tilde{q}_y')\,\mathrm{sinc}(\tilde{q}_y + \tilde{q}_y')\big] \end{aligned} \tag{10}$$

where

$$\Phi(\tilde{q}_x, \tilde{q}_y) = (l/\tilde{q})\mathrm{e}^{-\tilde{q}^2/4}. \tag{11}$$

The coefficients $\tilde{k}_i(\tilde{q}_x, \tilde{q}_y, \tilde{q}_y')$ ($i = 1, 2, 3$) can be determined by substituting the trial solution (10) into equation (9). The results, detailed in the appendix, are

$$\tilde{k}_3(\tilde{q}_x, \tilde{q}_y, \tilde{q}_y') \equiv -Xr_0/[\pi(1 + r_0\tilde{q}'\mathrm{e}^{-\tilde{q}'^2/2})] \tag{12}$$

$$\tilde{k}_i(\tilde{q}_x, \tilde{q}_y, \tilde{q}_y') = (-1)^{i+1} - \alpha_0(1+\alpha_0\tilde{K}_i)^{-1}C_1(\tilde{q}_x, \tilde{q}_y)C_2(\tilde{q}_x, \tilde{q}_y') \qquad (+\colon i = 1; -\colon i = 2) \tag{13}$$

where

$$\tilde{K}_\pm(\tilde{q}_x) \approx K_\pm(\tilde{q}_x) - \frac{r_0}{2}\int_{-\infty}^{\infty}\mathrm{d}\tilde{q}_y\;\mathrm{e}^{-\tilde{q}^2}\frac{1 \pm \cos 2\tilde{k}_F\tilde{q}_y}{2 + r_0\tilde{q}\mathrm{e}^{-\tilde{q}^2/2}}. \tag{14}$$

X is a fitting factor and the functions C_1 and C_2 are defined in the appendix; cf. equation (A.10).

Agreement with the numerical solution of equation (9) is obtained if we take

$$X = (2/\pi)\arctan[\tilde{q}_x^4 \exp(5\tilde{q}_x + 4.5)].$$

Another expression that gives a very good agreement is

$$X = 1 - \exp(-200\tilde{q}_x^4).$$

This means that for $\vec{q} = 0$ the interlevel contribution to the screened field is zero, while the intralevel one tends to infinity. Further, C_1 and C_2 have different forms because the screening in the QW is inhomogeneous along the y-direction. Equation (14) will be used in the next section.

3.2. Numerical solution and results

In principle, equation (9) can be solved by iteration. However, as the integral kernel on the right-hand side (RHS) of equation (9) becomes very large when q_x is very small, any small deviation in the trial values would cause a very large deviation on the RHS and lead to either divergent results or an extremely long procedure. We avoided these problems by taking the approximate analytical solution, equation (10), as the initial value and applying a 'weighted' iterative method. The details are as follows.

Suppose V_l^i is the LHS value obtained by substituting the trial value of the ith iteration V^i into the RHS of equation (9). Then the trial value of the $(i+1)$th iteration is taken as

$$V^{i+1} = V^i + x(V_l^i - V^i)$$

where $0 \leqslant x \leqslant 1$ is the 'weight' factor. If we take $x = 0$ we have $V^{i+1} = V^i$, which means that there is no change between successive iterations. On the other hand, if we take $x = 1$ we have $V^{i+1} = V_l^i$ as in the traditional iterative method. For equation (9) we take x small, say 0.5% for $q_x = 1/150$, to avoid divergence of results between iterations. In this way one can obtain the numerical solution with any accuracy, provided that the iteration times are large enough.

The results of the numerical solution of equation (9) are plotted in figures 1 and 2 for some special values of q_x and ω_c/Ω. For comparison the results of the approximate analytical solution, expressed by equations (10), (12), and (13), are shown by the dotted curves. As can be seen, the two results agree very well and this holds for large ranges of the parameters. For example, the value of ω_c/Ω can be changed, at least from 25 to 45, and that of $\tilde{q}_x$ from the very small value $0.1/\tilde{k}_F$ to the very large one $\tilde{k}_F$. Figures 1(a) and 2(a) show the worst case: $\tilde{q}_x = 1/\tilde{k}_F$.

4. Exchange and correlation energies, group velocities

With the help of equations (5), (10), and (13), the correlation and exchange energies ($q_-^2 = \tilde{k}_-^2 + \tilde{q}_y^2$, $q'^2_- = \tilde{k}_-^2 + \tilde{q}_y'^2$, $Q_\pm = \tilde{k}_x - \tilde{k}_-/2 \pm \tilde{k}_F$) can be written as

$$\varepsilon^{co}_{0,k_x,1} \approx \frac{r_0\hbar\tilde{\omega}}{2\pi}\int_{\tilde{k}_x-\tilde{k}_F}^{\tilde{k}_x+\tilde{k}_F} \mathrm{d}\tilde{k}_- \left[\sum_{+,-}\frac{\alpha_0}{1+\alpha_0\tilde{K}_\pm(\tilde{k}_-)}F_{\pm,1}F_{\pm,2} + G\right] \tag{15}$$

where

$$F_{\pm,i} = \int_{-\infty}^{\infty}\frac{\mathrm{d}\tilde{q}_y\ \mathrm{e}^{-q_-^2/2}}{2q_-}C_i\left[\cos(Q_-\tilde{q}_y) \pm \cos(Q_+\tilde{q}_y)\right] \qquad i = 1, 2 \tag{16}$$

$$G = \int_{-\infty}^{\infty}\int_{-\infty}^{\infty}\mathrm{d}\tilde{q}_y\ \mathrm{d}\tilde{q}_y'\ \frac{\mathrm{e}^{-(q_-^2+q'^2_-)/2}}{q_-q'_-}\tilde{k}_3\cos[(\tilde{q}_y+\tilde{q}_y')(\tilde{k}_x-\tilde{k}_-/2)]\,\mathrm{sinc}(\tilde{q}_y+\tilde{q}_y') \tag{17}$$

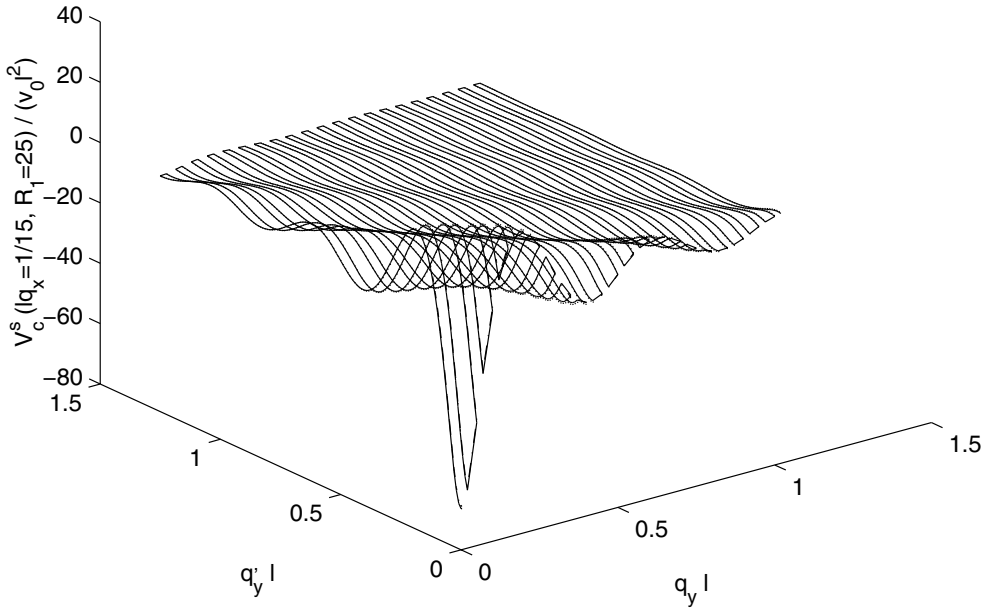

(a)

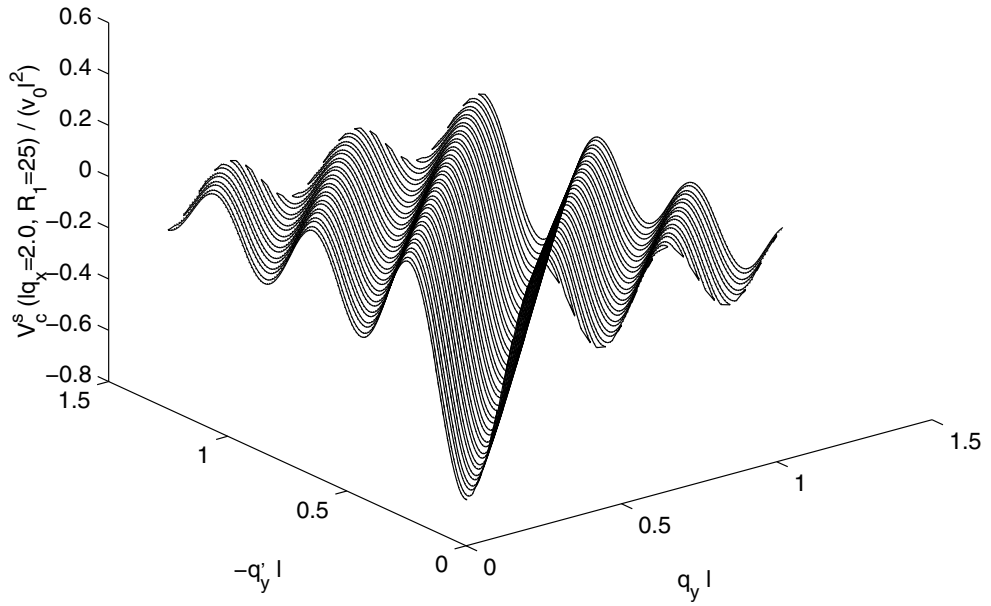

(b)

Figure 1. The numerical solutions (solid lines) and the approximate solutions (dotted lines) of equation (9) for $q_x l = 1/\tilde{k}_F = 1/15$ (a) and $q_x l = 2.0$ (b) for $r_0 = 0.85$, $R_1 = \omega_c/\Omega = 25$.

and

$$\varepsilon^{ex}_{0,k_x,1} = -\frac{r_0\hbar\tilde{\omega}}{2\pi}\left(\int_0^{\tilde{k}_F+\tilde{k}_x} \mathrm{d}\tilde{k}_- + \int_0^{\tilde{k}_F-\tilde{k}_x} \mathrm{d}\tilde{k}_-\right)\int \mathrm{d}\tilde{q}_y \, \frac{\mathrm{e}^{-q_-^2/2}}{q_-}. \tag{18}$$

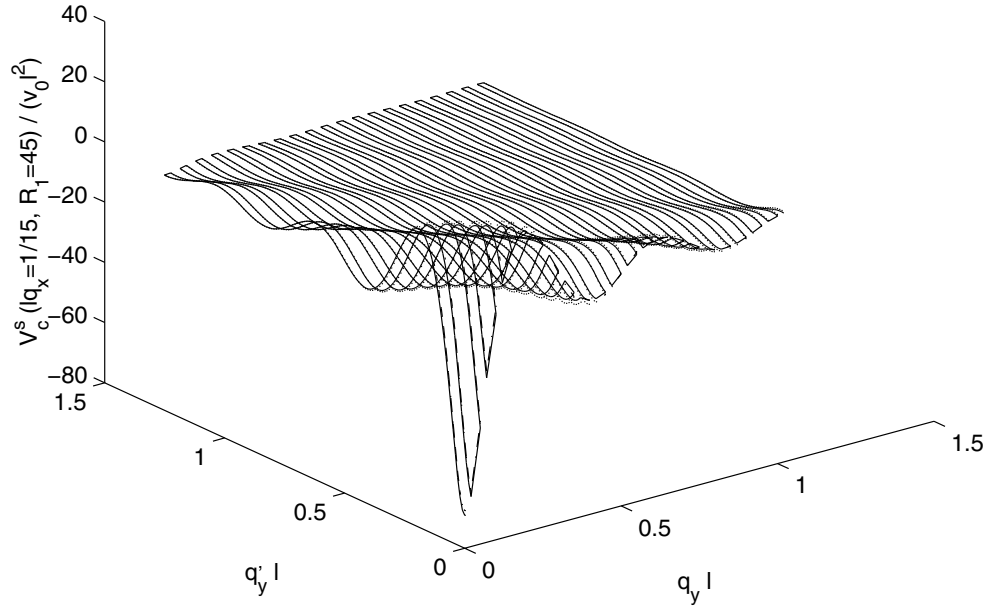

(a)

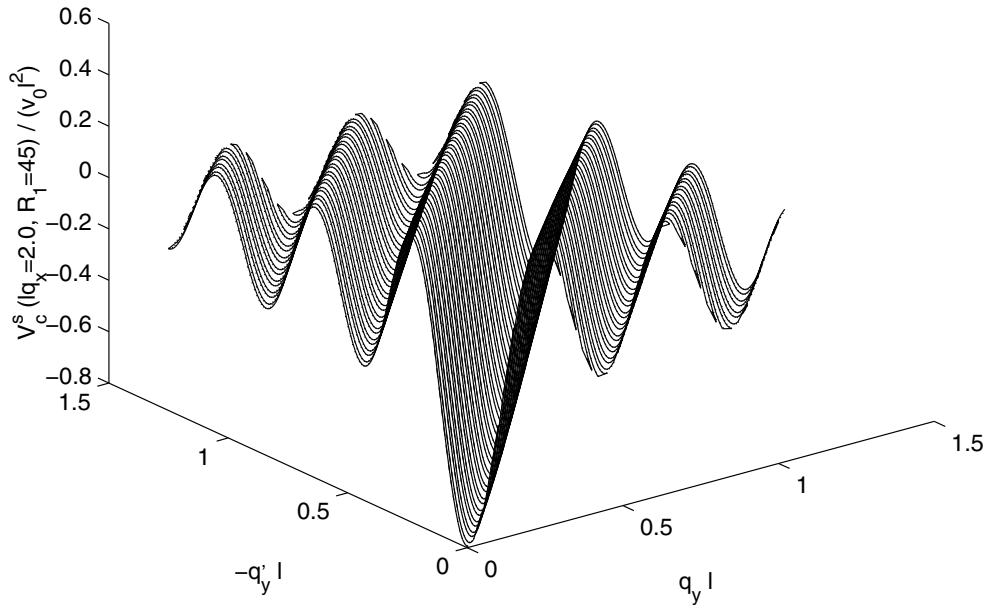

(b)

Figure 2. As figure 1, but for $q_x l = 1/\tilde{k}_F$ (a) and $q_x l = 2.0$ (b) with $r_0 = 1.0$, $R_1 = \omega_c/\Omega = 45$.

In equation (15) the last term is the correlation contribution from the neighbouring level. The total correction to the free-particle energy due to exchange and correlations, $\varepsilon^{ec}_{0,k_x,1}$, is given by the sum of the contributions from equations (15) and (18).

To study the behaviour of the exchange and correlations near the Fermi edge we consider

the derivative

$$v_g^{ec}(k_F) = \frac{l}{\hbar}\frac{\partial}{\partial \tilde{k}_x}\varepsilon^{ec}_{0,k_x,1}\bigg|_{k_x\to k_F}$$
$$= \frac{l\tilde{\omega}r_0}{2\pi}\left[K_0\left(\frac{\tilde{k}_0^2}{4}\right) - \frac{\alpha_0 K_+(\tilde{k}_0)\tilde{K}_+(\tilde{k}_0)}{1+\alpha_0\tilde{K}_+(\tilde{k}_0)} - \frac{\alpha_0 K_-(\tilde{k}_0)\tilde{K}_-(\tilde{k}_0)}{1+\alpha_0\tilde{K}_-(\tilde{k}_0)}\right]\bigg|_{\tilde{k}_0\to 0} \tag{19}$$

where $\tilde{k}_0 = \tilde{k}_F - \tilde{k}_x$. Making the approximations, for $\alpha_0\tilde{K}_\pm > 1$, $K_0(x)|_{x\to 0} \approx \ln(2/x)$ and $\alpha_0\tilde{K}\pm/(1+\alpha_0\tilde{K}_\pm) \approx 1 - 1/\alpha_0\tilde{K}_\pm(\tilde{k}_0)$, and using equation (14), we can simplify equation (19) further and obtain

$$v_g^{ec}|_{\tilde{k}_0\to 0} = \frac{l\tilde{\omega}r_0}{2\pi}\left[K_0\left(\frac{\tilde{k}_0^2}{4}\right) - \left(1 - \frac{1}{\alpha_0\tilde{K}_+}\right)K_+ - \left(1 - \frac{1}{\alpha_0\tilde{K}_-} + \left(\frac{1}{\alpha_0\tilde{K}_-}\right)^2\right)K_-\right]$$
$$= \frac{l\tilde{\Omega}}{2}\left(\frac{\Omega}{\tilde{\omega}}\tilde{k}_F\right)\left[\frac{K_+}{\tilde{K}_+} + \frac{K_-}{\tilde{K}_-} - \frac{K_-}{\alpha_0\tilde{K}_-^2}\right]. \tag{20}$$

The first term on the first line of equation (20) comes from the exchange; it is positive and logarithmically divergent for $\tilde{k}_0 \to 0$. However, its singularity is cancelled exactly by that of the correlations. This conclusion can be proved to be true even when the condition $\alpha_0\tilde{K}_\pm > 1$ is not satisfied. Also, one can see from equations (17) and (19) that near the Fermi edge the adjacent-level contribution to the derivative $\partial\varepsilon^{ec}_{0,k_x,1}/\partial\tilde{k}_x$ tends to zero very quickly. In this case the nonsingular part of the total derivative comes from intralevel screening. For strong magnetic fields, $v_g^{ec}(k_F)$ given by equation (20) tends to be a constant:

$$v_g^{ec}(k_F) = v_g^H\left[1 + \frac{1}{\tilde{K}_-}\frac{r_0}{4}\int_{-\infty}^{\infty}\frac{\mathrm{d}\tilde{q}_y\,\mathrm{e}^{-\tilde{q}_y^2}(1-\cos 2\tilde{k}_F\tilde{q}_y)}{2 + r_0\sqrt{\tilde{k}_0^2+\tilde{q}_y^2}\,\mathrm{e}^{-(\tilde{k}_0^2+\tilde{q}_y^2)/2}}\right] \approx v_g^H(k_F) \tag{21}$$

where $v_g^H(k_F) = l\tilde{\Omega}(\Omega\tilde{k}_F/\tilde{\omega})$. This conclusion is reached because the second term in the square brackets is less than 4% of the first term, e.g., for $r_0 = 1$, and is consistent with the approximate result of reference [6].

5. Concluding remarks

In section 4 we obtained, within the SHFA, the exchange–correlation energy $\varepsilon^{ec}_{0,k_x,1}$ and its contribution to the Fermi-edge group velocity. Our derivation is based on the approximate solution of the integral equation for the screened potential. As shown in section 3, this approximate solution, which served as a very good first step for the iteration procedure, agrees very well with the numerical one. Another important point is that, in contrast with standard perturbative calculations or those of reference [6], in our approach making the assumption $r_0 \ll 1$ is not necessary.

We further notice that, as in reference [6], for the single-particle energy $E_{n,k_x,\sigma}$ the results can be described in the framework of the local-density approximation (LDA) [12]. The latter can be calculated at $T = 0$ by solving the single-particle Schrödinger equation

$$[h^0 + V_{xc}(y)]|\varphi\rangle = E_{n,k_x,\sigma}|\varphi\rangle \tag{22}$$

where $V_{XC}(y)$ is the effective potential. The corresponding eigenvalue can be obtained from $E_{0,k_x,1} = \varepsilon_{0,k_x,1} + \langle|V_{XC}(y)|\rangle$, since $V_{XC}(y)$ is small compared to $\hbar^0$. Now as in reference [6] we take

$$V_{XC}(y) \approx \varepsilon^{ec}_{0,y/l^2,1} = \varepsilon^{ec}_{0,k_x,1} \qquad |y| \leqslant y_0(k_F). \tag{23}$$

As for the region $|y| > y_0(k_F)$, we take $V_{XC}(y) = 0$. Then upon evaluation of $\langle|V_{XC}(y)|\rangle$ we find a very good agreement with the results of section 3 for the energies.

We now apply our theory to the experimental situation of reference [5] in GaAlAs/GaAs QWs. The parameters for sample 1 are $\hbar\Omega \approx 0.65$ meV, $B \approx 10$ T, $W \approx 0.30$ μm; this gives $\tilde{k}_F \approx 15$, $\omega_c/\Omega \approx 25$. For sample 2, the estimated parameters are $\hbar\Omega = 0.46 \pm 0.2$ meV, $B \approx 7.3$ T, $W \approx 0.33$ μm, and they lead to $\tilde{k}_F \approx 15$ and $\omega_c/\Omega \approx 32$. We plot our results for sample 1 and sample 2 in figures 3 and 4, respectively. Figure 3 shows that electronic correlations suppress the spin splitting and therefore there is no $\nu = 1$ quantum Hall-effect (QHE) state in sample 1. In figure 4, at the Fermi edge, there is an activation gap $\Delta E_{\downarrow F} \approx 0.013\hbar\omega_c \approx 1.5$ K. This is very close to the experimental result [5] $\Delta E_{\downarrow F} \approx 1$ K. The single-particle group velocity at the Fermi level $v_g(k_x) = (1/\hbar)(\partial/\partial\tilde{k}_x)E_{0,k_x,1}$ can be calculated as

$$v_g(k_F) = v_g^H(k_F) + \frac{l}{\hbar}\frac{\partial}{\partial\tilde{k}_x}\langle|\varepsilon^{ec}_{0,k_x,1}|\rangle|_{\tilde{k}_x\to\tilde{k}_F}. \tag{24}$$

A numerical calculation gives $v_g(k_F) = 6.9v_g^H$ and $v_g(k_F) \approx 11v_g^H$ for samples 1 and 2, respectively. The corresponding values of reference [6] are, respectively, $v_g(k_F) = 10v_g^H$ and $v_g(k_F) = 5v_g^H$.

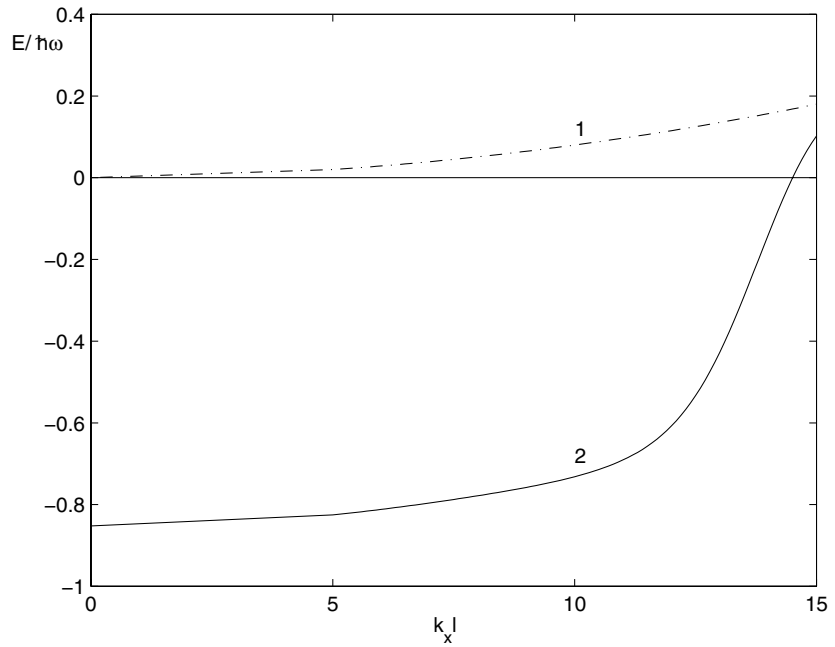

Figure 3. Energies as a function of $\tilde{k}_x$ for sample 1 of reference [5]. The parameters are $\hbar\Omega \approx 0.65$ meV, $B \approx 10$ T, $W \approx 0.30$ μm, $\tilde{k}_F \approx 15$, and $R_1 = \omega_c/\Omega \approx 25$. Curve 1 shows $E = \varepsilon_{0,k_x,-1}$ for the upper spin-split LL. Curve 2 shows $E = \varepsilon_{0,k_x,1} + \varepsilon^{ec}_{0,k_x,1}$ obtained from equations (2), (15), and (18). Notice that there is no finite gap that would lead to the $\nu = 1$ QHE.

In summary, we have assessed the effects of Coulomb interaction and correlations in quantum wires at strong magnetic fields for $\nu = 1$. We have obtained an overall agreement between the analytical and numerical results as well as between the theoretical and the experimental results. Actually, the approach we that we discussed in section 3, involving

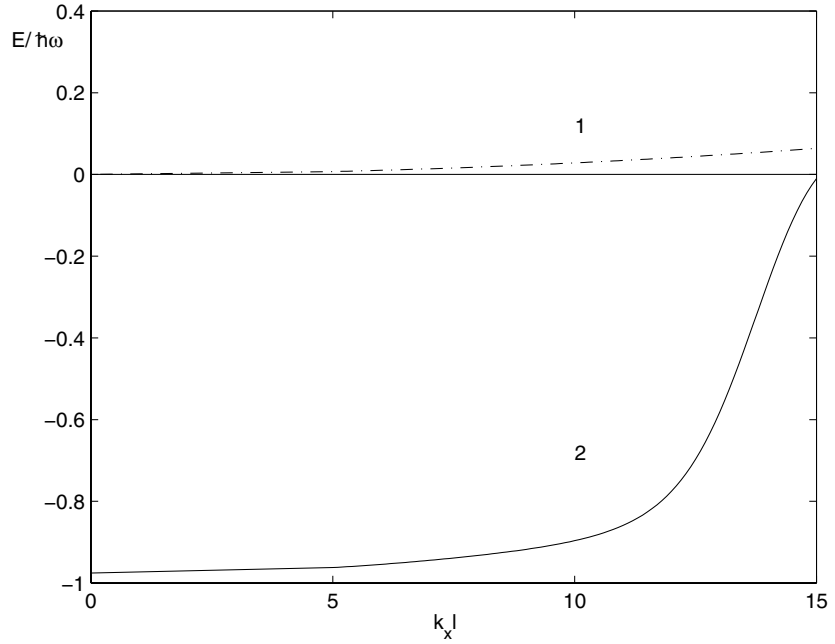

Figure 4. As figure 3, but with the parameters of sample 2 of reference [5], i.e. $\hbar\Omega = 0.46 \pm 0.2$ meV, $B \approx 7.3$ T, $W \approx 0.33$ μm, $\tilde{k}_F \approx 15$, and $R_1 = \omega_c/\Omega \approx 32$. In contrast with figure 3, when the exchange and correlations are taken into account, a gap appears between the curves for the $\sigma = -1$ and $\sigma = 1$ LLs and leads to the $\nu = 1$ QHE state.

only interlevel and adjacent-level screening, can also be applied to the cases of $\nu = 2, 3$, provided that $\tilde{k}_F^{\nu}$ is large enough. This will be the subject of a separate investigation.

Acknowledgments

We thank Dr O G Balev for a critical reading of an earlier version of the manuscript and useful suggestions. This work was supported by the Canadian NSERC Grant No OGP0121756.

Appendix A. Solution of the integral equation

To solve equation (9) we make the approximation

$$(2\tilde{m}/\hbar^2)\int_{-k_F}^{-k_F+q_x} \mathrm{d}k_{x\alpha}\,\frac{\mathrm{e}^{-\mathrm{i}a(\tilde{q}_y+\tilde{q}_y')\tilde{k}_{x\alpha}}}{(k_{x\alpha}-q_x)^2-k_{x\alpha}^2}$$
$$= (v_1\tilde{k}_F/\tilde{q}_x)\mathrm{e}^{-\mathrm{i}a(\tilde{q}_y+\tilde{q}_y')\tilde{q}_x/2}\left[E_i(A_-)-E_i(A_+)\right] \quad (A.1)$$
$$\approx v_1\mathrm{e}^{\mathrm{i}a(\tilde{q}_y+\tilde{q}_y')(\tilde{k}_F-\tilde{q}_x/2)} \quad (A.2)$$

where $A_\pm = \mathrm{i}(\tilde{q}_y + \tilde{q}_y')(\tilde{k}_F \pm \tilde{q}_x/2)$, $v_1 = -\tilde{m}/\hbar^2 k_F = -(\tilde{\omega}/\Omega)^2(1/\tilde{k}_F l\hbar\tilde{\omega})$ and E_i is the exponential integral [10]. In equation (A.1) we can neglect the change in amplitude because it has a very small effect on the screened field described by equation (6) and on the exchange and correlation energy given by equation (5). However, the variation in phase caused by different $\tilde{q}_x$ plays a much more important role in equation (5). To simplify the results, we make the

approximation (A.2). Also, in agreement with experiments [5], we take $\tilde{k}_F = 15$. This is sufficiently large to allow the use of the simplified equation (9) for studying the exchange and correlation in our problem. For simplicity we use $a \approx 1$.

We now substitute the trial solution (10) in equation (9). With the help of $\mathrm{sinc}(x) \sim \delta(x)$ and the neglect of small oscillatory terms, we can make the following approximations:

$$\int \mathrm{d}\tilde{q}_{y1}\, \frac{\mathrm{e}^{-\tilde{q}_1^2/2}}{\tilde{q}_1} \tilde{k}_3(\tilde{q}_x, \tilde{q}_{y1}, \tilde{q}'_y)(\tilde{q}_x^2 - \tilde{q}'_y\tilde{q}_{y1})\,\mathrm{sinc}(\tilde{q}'_y + \tilde{q}_{y1}) \cos \tilde{k}_F\tilde{q}_{y1}$$
$$\approx \frac{\pi}{2}\tilde{k}_3(\tilde{q}_x, -\tilde{q}'_y, \tilde{q}'_y)\tilde{q}'\mathrm{e}^{-\tilde{q}'^2/2} \cos \tilde{k}_F\tilde{q}'_y \tag{A.3}$$

$$\int \mathrm{d}\tilde{q}_{y1}\, \frac{\mathrm{e}^{-\tilde{q}_1^2/2}}{\tilde{q}_1} \tilde{k}_3(\tilde{q}_x, \tilde{q}_{y1}, \tilde{q}'_y)(\tilde{q}_x^2 - \tilde{q}'_y\tilde{q}_{y1})\,\mathrm{sinc}(\tilde{q}'_y + \tilde{q}_{y1}) \sin \tilde{k}_F\tilde{q}_{y1}$$
$$\approx \frac{\pi}{2}\tilde{k}_3(\tilde{q}_x, -\tilde{q}'_y, \tilde{q}'_y)\tilde{q}'\mathrm{e}^{-\tilde{q}'^2/2} \sin \tilde{k}_F\tilde{q}'_y \tag{A.4}$$

$$\int \mathrm{d}\tilde{q}_{y1} \frac{\mathrm{e}^{-\tilde{q}_1^2/2}}{\tilde{q}_1} \tilde{k}_3(\tilde{q}_x, \tilde{q}_{y1}, \tilde{q}'_y)(\tilde{q}_x^2 - \tilde{q}'_y\tilde{q}_{y1})(\tilde{q}_x^2 + \tilde{q}_y\tilde{q}_{y1})\,\mathrm{sinc}(\tilde{q}_y - \tilde{q}_{y1})\,\mathrm{sinc}(\tilde{q}'_y + \tilde{q}_{y1})$$
$$\approx \pi\tilde{k}_3(\tilde{q}_x, \tilde{q}_y, \tilde{q}'_y)(\tilde{q}_x^2 - \tilde{q}'_y\tilde{q}_y)\tilde{q}\mathrm{e}^{-\tilde{q}^2/2}\,\mathrm{sinc}(\tilde{q}'_y + \tilde{q}_y). \tag{A.5}$$

If we now equate the coefficients of the $\cos \tilde{k}_F\tilde{q}_y \cos \tilde{k}_F\tilde{q}'_y$, $\sin \tilde{k}_F\tilde{q}_y \sin \tilde{k}_F\tilde{q}'_y$, and $\mathrm{sinc}(\tilde{q}_y + \tilde{q}'_y)$ terms on both sides of equation (9) we obtain

$$\tilde{k}_3(\tilde{q}_x, \tilde{q}_y, \tilde{q}'_y) = -\frac{r_0}{\pi}\left[1 + \pi\tilde{q}'\mathrm{e}^{-\tilde{q}'^2/2}\tilde{k}_3(\tilde{q}_x, \tilde{q}_y, \tilde{q}'_y)\right] \tag{A.6}$$

$$\tilde{k}_i(\tilde{q}_x, \tilde{q}_y, \tilde{q}'_y) = \mp\alpha_0\left[1 \pm \int_{-\infty}^{\infty} \mathrm{d}\tilde{q}_{y1}\, \frac{\mathrm{e}^{-\tilde{q}_1^2/2}}{\tilde{q}_1} \frac{1 \pm \cos(2\tilde{k}_F\tilde{q}_{y1})}{2} \tilde{k}_i(\tilde{q}_x, \tilde{q}'_y, \tilde{q}'_y)\right]$$
$$\mp r_0\frac{\alpha}{2}\tilde{q}'\mathrm{e}^{-\tilde{q}'^2/2}\tilde{k}_3(\tilde{q}_x, -\tilde{q}'_y, \tilde{q}'_y) - \frac{r_0}{2}\tilde{q}\mathrm{e}^{-\tilde{q}^2/2}\tilde{k}_i(\tilde{q}_x, \tilde{q}_y, \tilde{q}'_y) \qquad i = 1, 2 \tag{A.7}$$

where $\alpha = (\tilde{\omega}/\Omega)^2(1/\tilde{k}_F)$ and $\alpha_0 = r_0\alpha/\pi$. The solution to equation (17) is

$$\tilde{k}_3(\tilde{q}_x, \tilde{q}_y, \tilde{q}'_y) = -r_0/[\pi(1 + r_0\tilde{q}'\mathrm{e}^{-\tilde{q}'^2/2})]. \tag{A.8}$$

This value of $\tilde{k}_3$ and those of $\tilde{k}_i$ $(i = 1, 2)$ given below with $X = 1$ lead to an expression for the potential that agrees with the numerical solution of equation (9), depending on the value of q_x, to within 80%–99%. A much better agreement is obtained if we change $\tilde{k}_3$ to $X\tilde{k}_3$ where X is a function of q_x; see below. As for $\tilde{k}_i$ $(i = 1, 2)$, we assume that it can be factorized as $\tilde{k}_i = \tilde{k}_{ix}(\tilde{q}_x)\tilde{k}_{iy}(\tilde{q}_x, \tilde{q}_y)\tilde{k}'_{iy}(\tilde{q}_x, \tilde{q}'_y)$. With

$$\tilde{k}_3(\tilde{q}_x, \tilde{q}_y, \tilde{q}'_y) \equiv -Xr_0/[\pi(1 + r_0\tilde{q}'\mathrm{e}^{-\tilde{q}'^2/2})] \tag{A.9}$$

we obtain

$$\tilde{k}_i(\tilde{q}_x, \tilde{q}_y, \tilde{q}'_y) = \frac{(-1)^{i+1} - \alpha_0}{1 + \alpha_0\tilde{K}_i} \frac{2}{2 + r_0\tilde{q}\mathrm{e}^{-\tilde{q}^2/2}}\left[1 - \frac{Xr_0\tilde{q}'\mathrm{e}^{-\tilde{q}'^2/2}}{2(1 + r_0\tilde{q}'\mathrm{e}^{-\tilde{q}'^2/2})}\right]$$
$$= \frac{(-1)^{i+1} - \alpha_0}{1 + \alpha_0\tilde{K}_i} C_1(\tilde{q}_x, \tilde{q}_y)C_2(\tilde{q}_x, \tilde{q}'_y) \qquad (+: i = 1; -: i = 2) \tag{A.10}$$

where

$$\tilde{K}_{\pm}(\tilde{q}_x) = \int_{-\infty}^{\infty} \frac{\mathrm{d}\tilde{q}_y\, \mathrm{e}^{-\tilde{q}^2/2}}{\tilde{q}(2 + r_0\tilde{q}\mathrm{e}^{-\tilde{q}^2/2})}(1 \pm \cos 2\tilde{k}_F\tilde{q}_y). \tag{A.11}$$

With $K_\pm = \tilde{K}_\pm|_{r_0=0}$ we have

$$K_\pm(\tilde{q}_x) \approx \left[\mathrm{e}^{\tilde{q}_x^2/4} K_0(\tilde{q}_x^2/4)/2 \pm K_0(2\tilde{k}_F\tilde{q}_x)\right] \mathrm{e}^{-\tilde{q}_x^2/2} \tag{A.12}$$

where $K_0(x)$ is the modified Bessel function [10] and

$$\begin{aligned}\tilde{K}_\pm(\tilde{q}_x) &= \int_{-\infty}^{\infty} \mathrm{d}\tilde{q}_y \, \frac{\mathrm{e}^{-\tilde{q}_y^2/2}}{\tilde{q}} \frac{1 \pm \cos 2\tilde{k}_F\tilde{q}_y}{2} \sum_{n=0} \left(-\frac{r_0}{2}\tilde{q}\mathrm{e}^{-\tilde{q}^2/2}\right)^n \\ &= K_\pm(\tilde{q}_x) - \frac{r_0}{2}\int_{-\infty}^{\infty} \mathrm{d}\tilde{q}_y \, \mathrm{e}^{-\tilde{q}^2} \frac{1 \pm \cos 2\tilde{k}_F\tilde{q}_y}{2 + r_0\tilde{q}\mathrm{e}^{-\tilde{q}^2/2}}. \end{aligned} \tag{A.13}$$

Substituting equations (A.9) and (A.10) back into equations (A.3)–(A.5) confirms the validity of these approximations.

References

[1] Dempsey J, Gelfand B Y and Halperin B I 1993 *Phys. Rev. Lett.* **70** 3639
Chklovskii D B, Shklovskii B I and Glazman L I 1992 *Phys. Rev.* B **46** 4026
Gelfand B Y and Halperin B I 1994 *Phys. Rev.* **49** 1862
Muller G, Weiss D, Khaetskii A V, von Klitzing K, Koch S, Nickel H, Schlapp W and Losch R 1992 *Phys. Rev.* **45** 3932

[2] Brey L, Palacios J J and Tejedor C 1993 *Phys. Rev.* B **47** 13 884

[3] Kinaret J M and Lee P A 1990 *Phys. Rev.* B **42** 11 768

[4] Suzuki T and Ando T 1993 *J. Phys. Soc. Japan* **62** 2986

[5] Wrobel J, Kuchar F, Ismail K, Lee K Y, Nickel H, Schlapp W, Grobecki G and Dietl T 1994 *Surf. Sci.* **305** 615

[6] Balev O G and Vasilopoulos P 1997 *Phys. Rev.* B **56** 6798

[7] Landau R H 1996 *Quantum Mechanics II* (Chichester: Wiley)

[8] Madelung O 1995 *Introduction to Solid-State Theory* (Berlin: Springer)

[9] Ando T and Uemura Y 1974 *J. Phys. Soc. Japan* **37** 1044

[10] *Table of Integrals, Series and Products* 1965 ed I S Gradshteyn and I M Ryzhik (New York: Academic)

[11] *Handbook of Mathematical Functions with Formulas, Graphs and Mathematical Tables* ed M Abramowitz and I A Stegun (New York: Dover)

[12] Kohn W and Vashishta P 1983 *Theory of The Inhomogeneous Electron Gas* ed S Lundqvist and N H March (New York: Plenum)